Archival Report

Biological Psychiatry: GOS

Antidepressant Response and Stress Resilience Are Promoted by CART Peptides in GABAergic Neurons of the Anterior Cingulate Cortex

Yuki Funayama, Haiyan Li, Erina Ishimori, Ayako Kawatake-Kuno, Hiromichi Inaba, Hirotaka Yamagata, Tomoe Seki, Shin Nakagawa, Yoshifumi Watanabe, Toshiya Murai, Naoya Oishi, and Shusaku Uchida

ABSTRACT

BACKGROUND: A key challenge in the understanding and treatment of depression is identifying cell types and molecular mechanisms that mediate behavioral responses to antidepressant drugs. Because treatment responses in clinical depression are heterogeneous, it is crucial to examine treatment responders and nonresponders in preclinical studies.

METHODS: We used the large variance in behavioral responses to long-term treatment with multiple classes of antidepressant drugs in different inbred mouse strains and classified the mice into responders and nonresponders based on their response in the forced swim test. Medial prefrontal cortex tissues were subjected to RNA sequencing to identify molecules that are consistently associated across antidepressant responders. We developed and used virus-mediated gene transfer to induce the gene of interest in specific cell types and performed forced swim, sucrose preference, social interaction, and open field tests to investigate antidepressant-like and anxiety-like behaviors.

RESULTS: *Cartpt* expression was consistently upregulated in responders to four types of antidepressants but not in nonresponders in different mice strains. Responder mice given a single dose of ketamine, a fast-acting non–monoamine-based antidepressant, exhibited high CART peptide expression. CART peptide overexpression in the GABAergic (gamma-aminobutyric acidergic) neurons of the anterior cingulate cortex led to antidepressant-like behavior and drove chronic stress resiliency independently of mouse genetic background.

CONCLUSIONS: These data demonstrate that activation of CART peptide signaling in GABAergic neurons of the anterior cingulate cortex is a common molecular mechanism across antidepressant responders and that this pathway also drives stress resilience.

https://doi.org/10.1016/j.bpsgos.2021.12.009

Typical antidepressants such as tricyclic antidepressants and selective serotonin and/or noradrenaline reuptake inhibitors, which are used for treating major depressive disorder (MDD), target monoamine systems that have widespread effects throughout the central nervous system. However, approximately 60% of patients do not respond to a single trial, and 30% to 40% of patients do not remit from depression even after multiple treatment attempts (1). Treatment responses in clinical depression vary, and treatment efficacy becomes evident after weeks or months, which necessitated the development of more effective treatments.

The prefrontal cortex (PFC) has emerged as a key brain region in MDD pathophysiology and in depression treatment (2–4). Neuroimaging studies of MDD have reported altered activity in the PFC (3,5–7). Clinical evidence suggests the involvement of PFC GABA (gamma-aminobutyric acid)–related molecules in MDD pathophysiology and antidepressant actions (8–11). Preclinical studies indicated that the medial PFC (mPFC), which includes the prelimbic cortex, infralimbic cortex, and anterior cingulate cortex (aCC), is associated with both depression-like behaviors and induction of antidepressant-like response in rodents (12–15). Thus, the mPFC may exert strong regulation over mood-related behaviors.

A key challenge in understanding and ultimately treating depression is identifying molecular mechanisms that mediate behavioral responses to antidepressants (16). As mentioned above, given that antidepressant responses vary widely among humans, it is important to stratify animals into subgroups of responders and nonresponders to antidepressant treatments to better understand the mechanism of action of antidepressant drugs. In addition, the genetic backgrounds of mice influence their sensitivity to antidepressants (17–19), whereas the common molecular mechanisms driving antidepressant-like behaviors across inbred mice strains remain unknown. Furthermore, it remains unclear whether there are common transcriptional signatures across multiple types of antidepressant drugs. Therefore, identifying molecules that are consistently regulated in multiple classes of antidepressant

ISSN: 2667-1743

responders and are commonly regulated in various inbred mouse strains may provide insight on the molecular mechanisms targeted by both established and experimental pharmacotherapies.

Herein, we developed an animal-based approach modeling the heterogeneity in response to long-term treatment with four classes of antidepressants in three mouse strains. Our data revealed fundamental differences in molecular signatures between responders and nonresponders and implicated specific molecules in the development of antidepressants.

METHODS AND MATERIALS

Additional information is available in Supplement 1.

Animals

All procedures were performed according to the Guide for Animal Care and Use of Yamaguchi University and Kyoto University and were approved by the Institutional Animal Care and Use Committees of Kyoto University and Yamaguchi University.

Antidepressant Treatment

For continuous treatment with imipramine hydrochloride (IMI), maprotiline hydrochloride (MPR), sertraline hydrochloride (SRT), and duloxetine hydrochloride (DLX), the drugs were dissolved in tap water to a concentration of 160 mg/L (17,20,21) and administered for 3 weeks (long-term) or 5 days (short-term). Vehicle-treated animals received drinking water regularly.

Social Defeat Stress

Chronic social defeat stress (CSDS) and subchronic and mild SDS were administered as reported previously (22–24).

Behavioral Tests

All behavioral experiments were performed between 9:00 AM and 3:00 PM in a blinded fashion as reported previously (21,23,25).

Forced Swim Test. Mice were placed in a cylinder of water and allowed to swim around freely for 6 minutes, and their immobility time was measured.

Sucrose Preference Test. After a 16-hour liquid deprivation, mice were given two bottles, one with 1.5% sucrose and another with tap water, for 4 hours. The sucrose preference was calculated as the percentage of sucrose solution consumed relative to the total intake.

Open Field Test. Mice were individually placed in the center of an open field box and allowed to explore the arena freely for 5 minutes. The percentage of time spent in the center area was measured automatically using an ANY-maze video-tracking system.

Social Interaction Test. Mice were placed in a test chamber with an empty wire-mesh cage as a first term for 3 minutes, then with an unfamiliar CD-1 mouse enclosed in the wire-mesh cage as a second term for 3 minutes. The time spent in the area surrounding the wire-mesh cage was measured in both sessions automatically using an ANY-maze tracking system.

RNA Analysis

Total RNA from mPFC regions, including the prelimbic cortex, infralimbic cortex, and aCC (bregma 1.98–0.98 mm) was extracted using the Direct-zol RNA Microprep according to the manufacturer's instructions (Zymo Research). An Illumina HiSeq system was used for RNA sequencing (RNA-seq). Raw data were deposited in the Gene Expression Omnibus (GSE168172). The sequences of all primers used in quantitative polymerase chain reaction (Q-PCR) are listed in Table S1 in Supplement 2. RNAscope from brain sections (anterior part of Cg1/Cg2, bregma 1.70–1.18 mm) was performed as described previously (23).

Statistical Analysis

Complete statistical summaries are provided in Table S2 in Supplement 3. GraphPad Prism (version 7.0; GraphPad Software Inc.) and SPSS Statistics (version 25; IBM Corp.) were used to perform Student t test, unpaired t test, Wilcoxon test, Kruskal-Wallis test, and one- or two-way analysis of variance as appropriate to determine statistical differences. For analysis of variance, significant effects were followed by Tukey's post hoc comparison. For multiple comparisons, Dunnett's test was used and adjusted p values were adopted. To assess data normality, Kolmogorov-Smirnov and/or Shapiro-Wilk tests were used. In all cases, comparisons were considered significant at $p < .05$. All data are presented as mean ± SEM.

RESULTS

Modeling Heterogeneity in Antidepressant Treatment Response

We aimed to identify molecule(s) promoting behavioral responses to antidepressants regardless of genetic background and antidepressant class. Therefore, we characterized antidepressant-like behaviors in BALB/c (BALB), C57BL/6J (B6), and DBA/2 (DBA) inbred mice after long-term treatment with IMI, MPR, SRT, and DLX as a tricyclic antidepressant, tetracyclic antidepressant, selective serotonin reuptake inhibitor, and selective noradrenaline reuptake inhibitor, respectively. We performed the forced swim test (FST), which is commonly used to assess the efficacy of antidepressant response in rodents (26–29), and measured immobility time on the day before treatment (FST-1) (Figure 1A). Mice were then treated with antidepressants or vehicle via drinking water for 21 days and subsequently subjected to a second FST (FST-2). The antidepressant response was determined as the percentage change in immobility time from baseline (FST-1). We found a strain difference in antidepressant response (Figure 1B–D). In BALB mice, IMI and SRT had a significant effect on percentage change in immobility time (Figure 1B), whereas in B6 and DBA mice, MPR and DLX had significant effects (Figure 1C, D).

Because there was a large individual difference in antidepressant response (Figure 1B–D), we estimated the response ratio by dividing the immobility time of FST-1 by that of FST-2

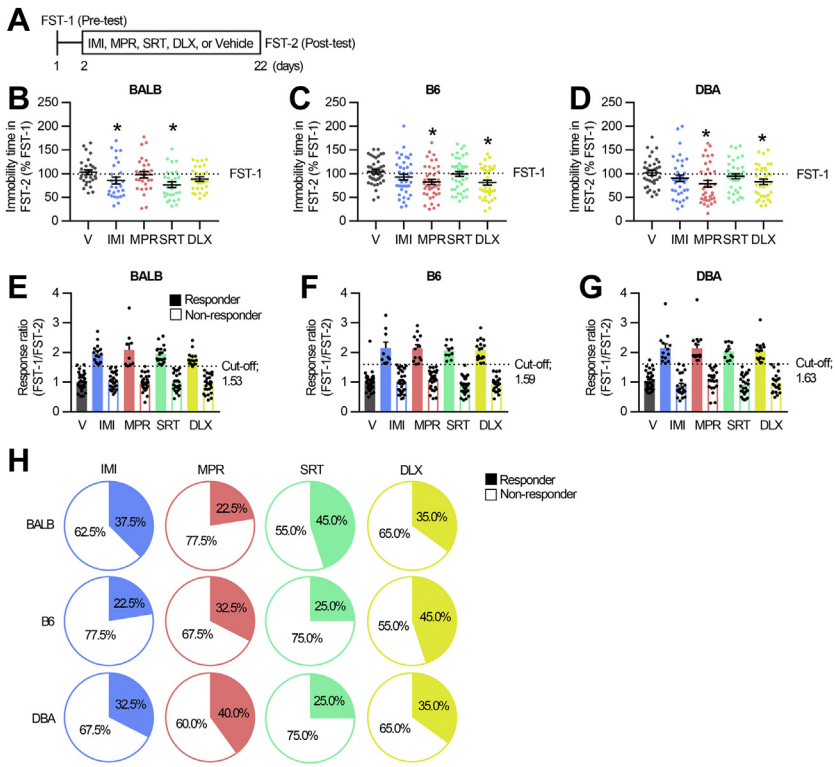

Figure 1. Identification of subgroups of responders and nonresponders to antidepressant treatments in inbred strains of mice. **(A)** Experimental design. Mice were tested using the FST-1 before a 3-week treatment with either tap water (V), IMI, MPR, SRT, or DLX. After long-term treatment with the antidepressant, a second FST (FST-2) was performed. **(B–D)** Immobility time in the FST-2 (% FST-1) in BALB/c (BALB) **(B)**, C57BL/6J (B6) **(C)**, and DBA/2 (DBA) **(D)** mice. $n = 36–40$ in each group. *$p < .05$ vs. FST-1 in the corresponding treatment. **(E–G)** Response ratio (immobility time in FST-1/immobility time in FST-2). The responder and nonresponder subgroups were identified by the mean + 2 SD method with a cutoff value. $n = 36–40$ in each group. **(H)** Distribution of responders and nonresponders in each strain of mice treated with specific antidepressants. $n = 36–40$ in each group. All data are presented as mean ± SEM. DLX, duloxetine; FST, forced swim test; IMI, imipramine; MPR, maprotiline; SRT, sertraline; V, vehicle.

and identified a treatment responder or nonresponder mouse with a cutoff value using a traditional mean ± 2 SD method. Mice with response ratios larger than the cutoff values (i.e., mean + 2 SD) in each strain were defined as responders (Figure 1E–G). The distribution pattern of the response to antidepressants significantly differed among strains, with overall 22.5% to 45% of the mice being responders to long-term antidepressant treatment (Figure 1H). In previous studies, nearly 30% of patients with MDD achieved remission after their first course of typical antidepressant pharmacotherapy (1,30), suggesting that our models could help provide translational and mechanistic insights into the mechanism of behavioral responses to antidepressants.

Differential Expression Signatures of Antidepressant Responders and Nonresponders

We performed RNA-seq to compare genome-wide transcriptional changes in responders and nonresponders. We selected the BALB strain because previous reports showed that this strain could be a stress-vulnerable model (21,23,31). In addition, we selected SRT and DLX for RNA-seq due to their increasing prescription worldwide (32,33). mPFC tissue punches from five BALB mouse groups were subjected to RNA-seq: SRT responders (SRT-R), SRT nonresponders (SRT-NR), DLX responders (DLX-R), DLX nonresponders (DLX-NR), and vehicle-treated mice. Differentially expressed genes (DEGs) were profiled in these conditions (Figure 2A; Table S3 in Supplement 4; Table S4 in Supplement 5; Table 5 in Supplement 6; Table S6 in Supplement 7; Table S7 in Supplement 8). We identified few common DEGs that were consistently upregulated in the SRT-R, SRT-NR, DLX-R, and DLX-NR groups relative to the vehicle. RNA-seq revealed that seven genes (*Nab2*, *Egr1*, *Egr2*, *Per1*, *c-fos*, *Otud1*, and *Dusp6*) were upregulated in both responders and nonresponders treated with SRT and DLX (Figure 2B; Table S3a in Supplement 4). This result was validated using Q-PCR (Figure 2C–I). We next identified DEGs that were upregulated/downregulated in either SRT-R, SRT-NR, DLX-R, or DLX-NR relative to the vehicle (Figure 2J–M; Table S3b in Supplement 4). The Gene Ontology profile analysis results at the biological process level of DEGs in each subgroup are shown in Figure 2N. Finally, we identified DEGs that were uniquely regulated in responders and nonresponders treated with SRT or DLX (Figure S1 in Supplement 1; Table S4 in Supplement 5).

Identification of Consistently Regulated Genes

A total of 65 DEGs were commonly regulated by SRT and DLX in responders (upregulated/downregulated in both SRT-R and DLX-R but not in SRT-NR or DLX-NR relative to the vehicle) (Figure 3A, B; Table S5a in Supplement 6). A total of 53 DEGs were commonly regulated by SRT and DLX in nonresponders (upregulated/downregulated in both SRT-NR and DLX-NR but not in SRT-R or DLX-R relative to the vehicle) (Figure S2 in Supplement 1; Table S5b in Supplement 6). Gene Ontology enrichment analysis revealed that genes that were consistently regulated in SRT and DLX responders were significantly enriched for the neuropeptide signaling pathway (Figure 3C, E), and network graphs showed that the gene encoding *Cartpt*

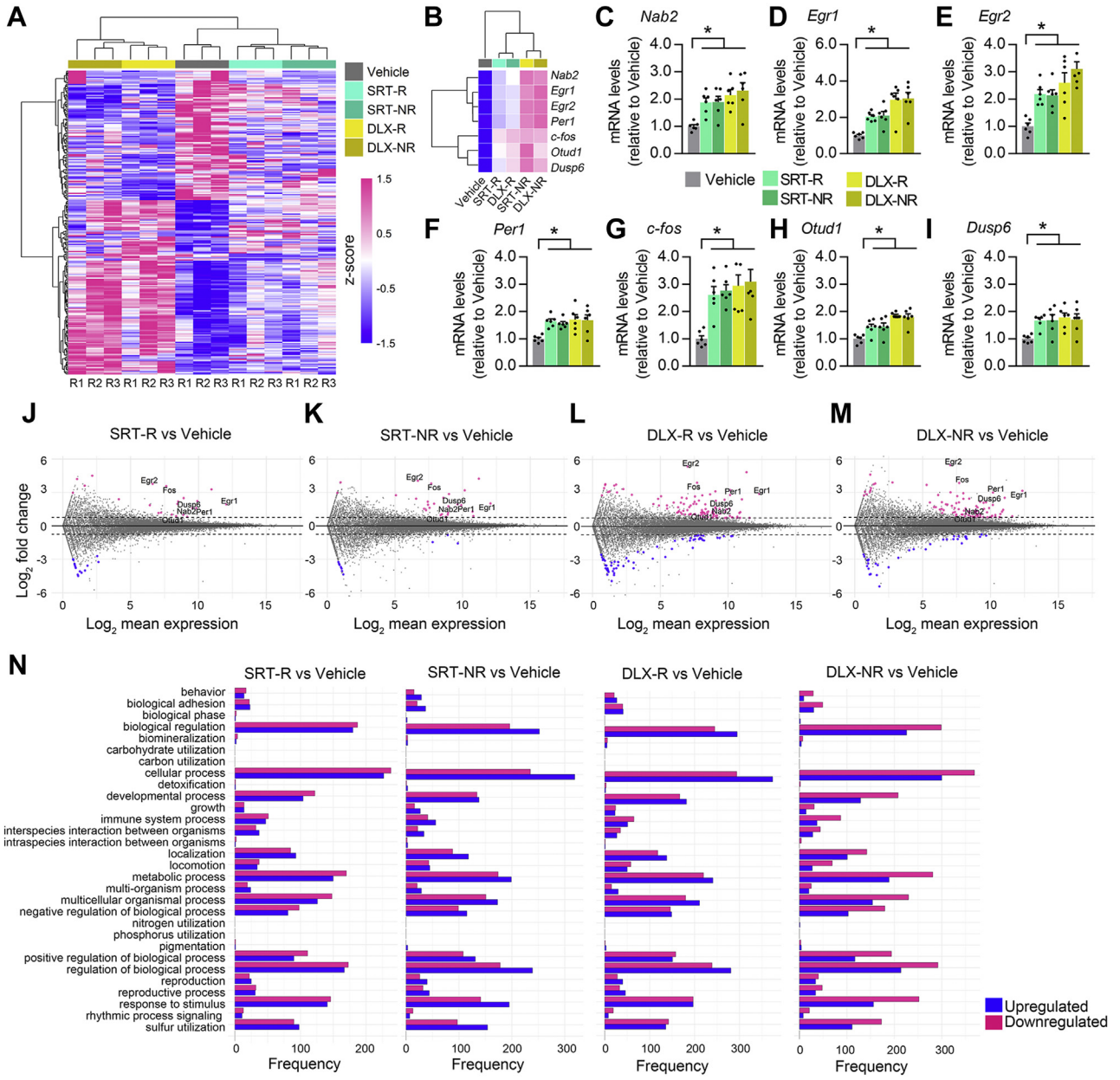

Figure 2. RNA sequencing reveals transcriptional alterations in the medial prefrontal cortex of antidepressant responders and nonresponders. **(A)** Heatmap representation of differentially expressed genes (fold change >1.3 and false discovery rate $p < .1$) in the responder and nonresponder groups to treatment with SRT and DLX (three replicates per group). **(B)** Heatmap representation of differentially expressed genes (fold change >1.3 and false discovery rate $p < .1$) that were commonly upregulated in both responders and nonresponders to treatment with SRT and DLX. **(C–I)** Real-time polymerase chain reaction validation of the alterations in gene expression identified in the differentially expressed gene analysis presented in **(B)**. $n = 6$ in each group. *Adjusted $p < .05$ vs. the vehicle. **(J–M)** MA plot of the results of the differential expression analysis in SRT-R **(J)**, SRT-NR **(K)**, DLX-R **(L)**, or DLX-NR **(M)**. **(N)** Gene Ontology profile analysis (biological process) of differentially expressed genes ($p < .05$) between the vehicle and SRT-R, SRT-NR, DLX-R, or DLX-NR (red, upregulated genes; blue, downregulated genes). The x-axis displays the number of differentially expressed genes, and the y-axis indicates the Gene Ontology terms. All data are presented as mean ± SEM. DLX-NR, DLX nonresponders; DLX-R, duloxetine responders; mRNA, messenger RNA; SRT-NR, sertraline nonresponders; SRT-R, sertraline responders.

was commonly implicated in SRT and DLX responders (Figure 3D, F). We then validated the messenger RNA (mRNA) expression of *Cartpt*, *Npas4*, *Col1a2*, *Col4a3*, *Creb3l4*, *CXCL16*, *Epn3*, and *Rsph6a*, which were DEGs consistently upregulated by SRT and DLX in responders in the RNA-seq analysis and were protein coding, mPFC-expressed genes (Allen Brain Atlas: http://mouse.brain-map.org/). Q-PCR results revealed the significantly altered expression of *Cartpt*, *Npas4*,

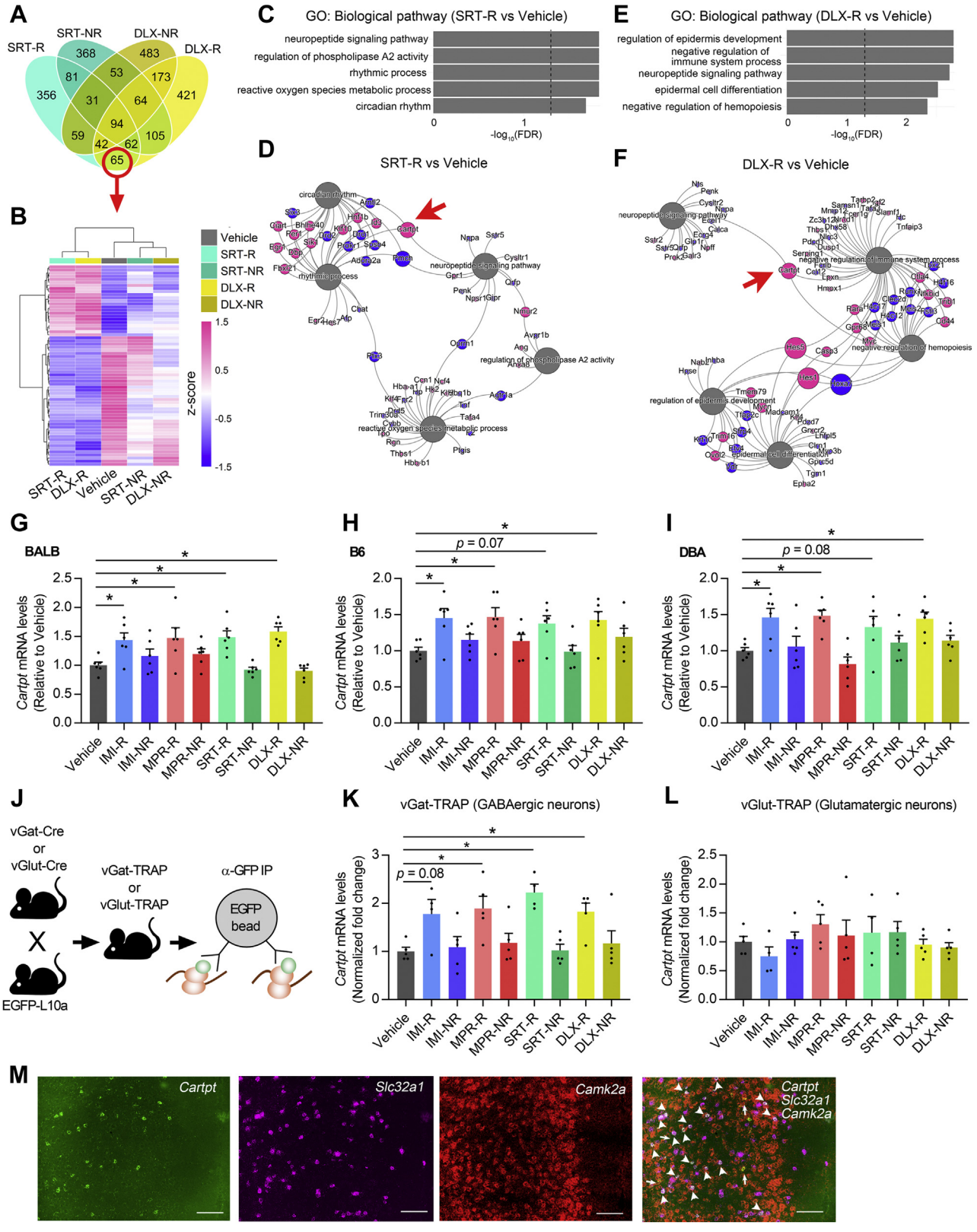
A
SRT-R
SRT-NR
DLX-NR
DLX-R
368
483
53
81
173
356
31
64
421
94
59
105
42
62
65
B
Vehicle
SRT-R
SRT-NR
DLX-R
DLX-NR
z-score
1.5
0.5
-0.5
-1.5
SRT-R
DLX-R
Vehicle
SRT-NR
DLX-NR
C
GO: Biological pathway (SRT-R vs Vehicle)
neuropeptide signaling pathway
regulation of phospholipase A2 activity
rhythmic process
reactive oxygen species metabolic process
circadian rhythm
-log10(FDR)
D
SRT-R vs Vehicle
E
GO: Biological pathway (DLX-R vs Vehicle)
regulation of epidermis development
negative regulation of immune system process
neuropeptide signaling pathway
epidermal cell differentiation
negative regulation of hemopoiesis
-log10(FDR)
F
DLX-R vs Vehicle
G
BALB
Cartpt mRNA levels (Relative to Vehicle)
H
B6
p = 0.07
I
DBA
p = 0.08
Vehicle
IMI-R
IMI-NR
MPR-R
MPR-NR
SRT-R
SRT-NR
DLX-R
DLX-NR
J
vGat-Cre or vGlut-Cre
X
EGFP-L10a
vGat-TRAP or vGlut-TRAP
α-GFP IP
EGFP bead
K
vGat-TRAP (GABAergic neurons)
Cartpt mRNA levels (Normalized fold change)
p = 0.08
L
vGlut-TRAP (Glutamatergic neurons)
M
Cartpt
Slc32a1
Camk2a
Cartpt
Slc32a1
Camk2a

Col1a2, *Epn3*, and *Rsph6a* in antidepressant-responder BALB, B6, or DBA mice (Figure 3G–I; Figure S3 in Supplement 1); among them, *Cartpt* expression was consistently and significantly upregulated in all antidepressant responders but not in nonresponders (Figure 3G–I). These findings suggest that neuropeptide signaling via CART peptides is associated with antidepressant response.

We also examined the effect of short-term antidepressant treatment on *Cartpt* mRNA expression in the aCC of B6 mice. After 5 days of DLX treatment, FST-2 was performed (Figure S4A in Supplement 1). There was no significant difference in immobility time between vehicle- and DLX-treated mice (Figure S4B in Supplement 1), and only 5 of 44 mice (11.4%) treated with DLX were responders (Figure S4C in Supplement 1). DLX-R mice exhibited a significantly higher *Cartpt* mRNA expression relative to vehicle-treated mice (Figure S4D in Supplement 1), suggesting that *Cartpt* induction promotes a behavioral response to antidepressants.

Ketamine, a fast-acting non–monoamine-based antidepressant, has emerged as a novel therapeutic agent. We tested whether ketamine upregulated *Cartpt* mRNA expression in the aCC of B6 mice. Consistent with a previous report (26), FST immobility time was significantly decreased 24 hours after ketamine treatment (Figure S5A–C in Supplement 1). *Cartpt* mRNA expression was significantly higher in ketamine treatment responders (48 hours after the ketamine injection) than that in the saline control (Figure S5D in Supplement 1). Collectively, these data suggest that CART peptide promotes the behavioral effects of traditional antidepressants and is associated with the antidepressant-like effects of ketamine.

CART Peptide Induction in GABAergic Neurons of the aCC of Antidepressant Responders

To identify specific cell types in which *Cartpt* expression is altered in antidepressant responders, we used the translating ribosome affinity purification (TRAP) technique, which enables identification of all proteins synthesized in a target cell population and alterations of this translational profile in response to pharmacological perturbations (34,35). vGat-Cre and vGlut-Cre mice were bred with transgenic mice expressing enhanced green fluorescent protein (EGFP)–tagged ribosomal protein L10a (EGFP-L10a) to establish vGat-TRAP and vGlut-TRAP mice. These mice expressed EGFP-L10a in GABAergic and glutamatergic neurons, respectively, enabling the identification of the cell type in which *Cartpt* expression is altered in responders (Figure 3J). vGat-TRAP and vGlut-TRAP mice were administered IMI, MPR, SRT, or DLX for 3 weeks and then divided into two groups (responders and nonresponders) based on their response ratio in the FST (Figure 1). Subsequently, EGFP-labeled polysomes from mouse mPFC tissue punches were affinity-purified to enrich cell-specific, polysome-bound, translating mRNAs. Q-PCR revealed that vGat-TRAP mice had significantly elevated *Cartpt* expression in GFP-immunoprecipitated samples in antidepressant responders, but not in nonresponders, when compared with vehicle-treated mice (Figure 3K). vGlut-TRAP mice did not show a significantly elevated *Cartpt* expression in GFP-immunoprecipitated samples in antidepressant responders (Figure 3L). These results suggest that *Cartpt* expression is induced in GABAergic neurons in antidepressant responders. For confirmation, we assessed *Cartpt* mRNA expression histologically using RNAscope. *Cartpt* mRNA was enriched in the aCC but was low or undetectable in the prelimbic and infralimbic areas (data not shown); moreover, in the aCC, the majority of *Cartpt*-expressing cells were *Slc32a1*-positive GABAergic neurons, with few *Cartpt*-expressing cells overlapping with *Camk2a*-positive glutamatergic neurons (Figure 3M). These results suggest that CART peptide signaling in GABAergic neurons of the aCC is associated with antidepressant response.

Effects of CART Peptide Overexpression in Antidepressant-like Behavior and Behavioral Response to Chronic Stress

To assess whether CART peptide induction in GABAergic neurons of the aCC is sufficient to induce an antidepressant-like behavior, we injected a Cre-dependent AAV (adeno-associated virus) expressing Cartpt (AAV-Cartpt) or control tdTomato (AAV-tdTomato) into the bilateral aCC of vGat-Cre or vGlut-Cre mice (C57BL/6J background) (Figure 4A). These mice were tested using FST under nonstress conditions and subjected to CSDS for 10 days; their behaviors were tested via the social interaction test (SIT), sucrose preference test, and open field test (Figure 4B). Histological analysis confirmed successful transgene expression in the aCC of vGat-Cre and vGlut-Cre mice (Figure 4C). Behaviorally, CART peptide overexpression in GABAergic neurons led to significantly decreased FST

Figure 3. Identification of *Cartpt* consistent upregulation across different types of antidepressant responders in three strains of mice. **(A)** Venn diagram indicating the number of differentially expressed genes across four comparisons SRT-R, SRT-NR, DLX-R, and DLX-NR and the overlap between the sets of genes. **(B)** Heatmap showing the 68 differentially regulated genes (fold change >1.3 and $p < .05$) that were consistently regulated in SRT and DLX treatment responders, but not in SRT or DLX treatment nonresponders. **(C–F)** GO enrichment analysis **(C, E)** and network graph visualization **(D, F)** of differentially expressed genes that were regulated in SRT **(C, D)** and DLX **(E, F)** treatment responders. Top five significant GO terms associated with differentially expressed genes in SRT-R and DLX-R. Note that the significant GO terms are associated with the neuropeptide signaling pathway (i.e., *Cartpt*) in responders to both antidepressant treatments. **(G–I)** Quantitative polymerase chain reaction revealing the upregulation of *Cartpt* in the medial prefrontal cortex of IMI-, MPR-, SRT-, and DLX responders, but not in their nonresponder counterparts in BALB/c (BALB) **(G)**, C57BL/6J (B6) **(H)**, and DBA/2 (DBA) **(I)** mice. $n = 4$–6 in each group. *Adjusted $p < .05$ vs. the vehicle. **(J)** TRAP strategy. EGFP-labeled polysomes were affinity-purified to enrich for glutamatergic or GABAergic neuron-specific, polysome-bound, translating mRNAs. **(K, L)** Quantitative polymerase chain reaction quantification of *Cartpt* expression in vGat-TRAP **(K)** and vGlut-TRAP **(L)** samples (relative to the vehicle). $n = 4$–5 samples in each group, and each sample was pooled from 4 to 6 mice (8–10 pairs of medial prefrontal cortex). *Adjusted $p < .05$. **(M)** RNAscope revealing that *Cartpt* expression (green) was enriched in the *Slc32a1*+ GABAergic neurons (magenta) but not in the *Camk2a*+ glutamatergic neurons (red) in the anterior cingulate cortex (Cg1/Cg2) of mice. The arrowheads and arrows indicate *Slc32a1*+ GABAergic neurons and *Camk2a*+ glutamatergic neurons, respectively. Scale bar = 100 μm. All data are presented as mean ± SEM. DLX-NR, duloxetine nonresponders; DLX-R, duloxetine responders; EGFP, enhanced green fluorescent protein; FDR, false discovery rate; GABAergic, gamma-aminobutyric acidergic; GO, Gene Ontology; IMI-NR, imipramine nonresponders; IMI-R, imipramine responders; IP, immunoprecipitation; MPR-NR, maprotiline nonresponders; MPR-R, maprotiline responders; mRNA, messenger RNA; SRT-R, sertraline responders; SRT-NR, sertraline nonresponders; TRAP, translating ribosome affinity purification.

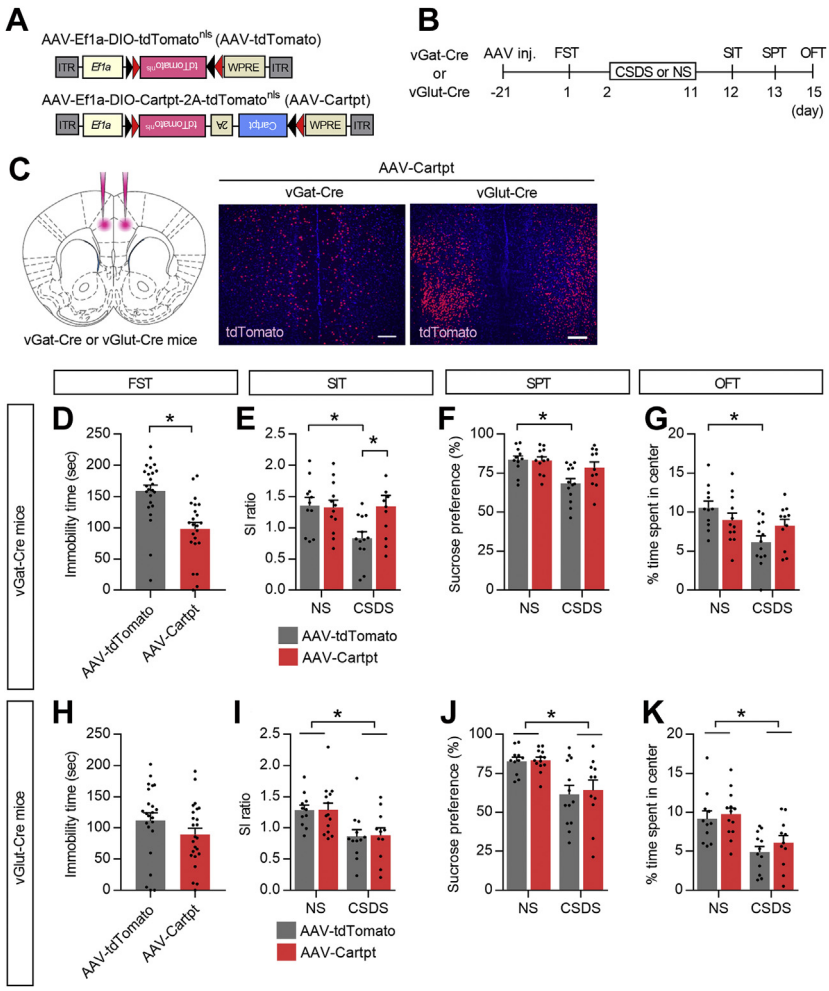

Figure 4. CART peptides in GABAergic neurons of the aCC drive antidepressant-like behaviors and stress resilience. **(A)** AAV vectors used for the control construct (AAV-tdTomato) and *Cartpt* overexpression (AAV-Cartpt). **(B)** Experimental paradigm of behavioral testing. **(C)** AAV microinjection into the aCC. Region-specific expression of tdTomato in the aCC is shown. Scale bar = 100 μm. **(D–G)** Effects of *Cartpt* overexpression in GABAergic neurons of the aCC on the FST **(D)**, SIT **(E)**, SPT **(F)**, and OFT **(G)**. n = 23–24 for FST and n = 11–13 for SIT, SPT, and OFT in each group. $^*p < .05$. **(H–K)** Effects of *Cartpt* overexpression in glutamatergic neurons of the aCC on the FST **(H)**, SIT **(I)**, SPT **(J)**, and OFT **(K)**. n = 23–24 for the FST and n = 11–14 for the SIT, SPT, and OFT in each group. $^*p < .05$. All data are presented as mean ± SEM. AAV, adeno-associated virus; aCC, anterior cingulate cortex; CSDS, chronic social defeat stress; FST, forced swim test; GABAergic, gamma-aminobutyric acidergic; inj. injection; NS, nonstress control; OFT, open field test; SIT, social interaction test; SPT, sucrose preference test.

immobility time (Figure 4D). Mice expressing control tdTomato showed significantly a decreased social interaction (SI) ratio in SIT, decreased sucrose preference in the sucrose preference test, and lower percent time spent in the center in the open field test after CSDS exposure when compared with nonstressed controls. In contrast, mice overexpressing CART peptide did not exhibit significant effects of CSDS (Figure 4E–G). Mice overexpressing CART peptide in glutamatergic neurons showed comparable behaviors to those of mice expressing control tdTomato in FST, and CART peptide overexpression did not affect any behavior in SIT, sucrose preference test, and open field test as animal models of depression (Figure 4H–K). These results suggest that CART peptide induction in GABAergic neurons of the aCC is sufficient for inducing an antidepressant-like behavior and chronic stress resiliency.

Behavioral Effects of CART Peptide Induction in GABAergic Neurons of the aCC in BALB/c Mice

We investigated whether the antidepressant response afforded by CART peptide is independent of mouse genetic background. First, we developed a novel inhibitory neuron-specific promoter with a length of 1.3 kb of the *Gad1* gene promoter and validated the specificity of this AAV. We injected AAVs expressing mCherry under the control of *Gad1* promoter (AAV-Gad1-mCherry) into the aCC of vGlut-Cre::GFP-L10a and vGat-Cre::GFP-L10a mice (Figure 5A). Histological analyses revealed that the majority of mCherry-positive cells colocalized with GFP-positive GABAergic neurons (77.8%) in vGat-Cre::GFP-L10a mice, whereas few mCherry-positive cells colocalized with GFP-positive glutamatergic neurons (5.1%) in vGat-Cre::GFP-L10a mice (Figure 5B, C).

Therefore, we injected either AAV-Gad1-Cartpt or AAV-Gad1-mCherry into the bilateral aCC region of BALB mice (Figure 5D). Three weeks after the surgery, the mice were subjected to FST and SIT in nonstress conditions, followed by re-evaluation of their behaviors in SIT after stress exposure (Figure 5E). Because BALB is susceptible to stress (21,23), we exposed the mice to a 5-day subchronic and mild SDS regimen, which is an abbreviated and subthreshold version of CSDS that is sufficient for

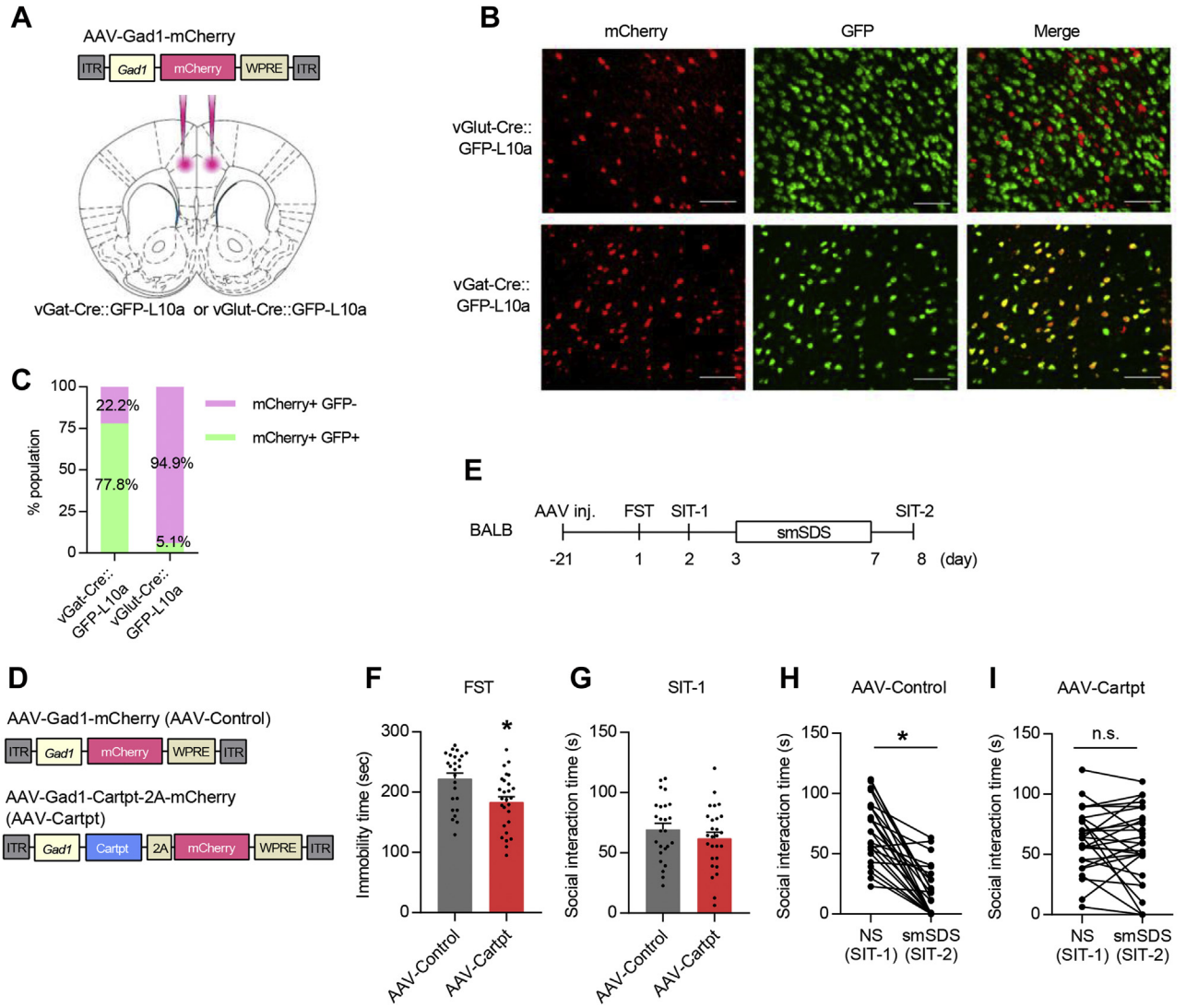

Figure 5. AAV-mediated CART peptide overexpression in aCC GABAergic neurons drives antidepressant-like behaviors and stress resilience in stress-vulnerable strains. **(A)** AAV vectors used for *mCherry* overexpression under the control of the *Gad1* promoter (AAV-Gad1-mCherry). To validate the cell-type specificity of the *Gad1* promoter in these AAVs, AAV-Gad1-mCherry was injected bilaterally into the aCC region of either vGat-Cre::GFP-L10a mice or vGlut-Cre::GFP-L10a mice (as reporter mice). **(B)** Fluorescence signals of EGFP (green) and mCherry (red) in the aCC of vGat-Cre::GFP-L10a mice (top panels) and vGlut-Cre::GFP-L10a mice (bottom panels). Colocalization of EGFP and mCherry is seen in vGat-Cre::GFP-L10a, but not in vGlut-Cre::GFP-L10a mice. Scale bar = 100 μm. **(C)** Quantification of the percentage of mCherry-positive cells (red) in the aCC region that overlap with GFP-positive cells (green). mCherry expression driven by the *Gad1* promoter is enriched in GFP-positive cells of vGat-Cre::GFP-L10a mice, but not of vGlut-Cre::GFP-L10a mice. $n = 4$ in each group; 425–685 mCherry-positive cells per group were analyzed. **(D)** AAV vectors used for *mCherry* (AAV-control) and *Cartpt* (AAV-Cartpt) overexpression under the control of the *Gad1* promoter. **(E)** Experimental paradigm used for behavioral testing. **(F)** Mice injected with AAV-Cartpt show reduced immobility time compared with mice injected with AAV-control in the FST. $n = 25–27$ in each group. $^*p < .05$. **(G)** Mice injected with AAV-Cartpt show a comparable SI time to that of mice injected with AAV-control in nonstressed conditions. $n = 25–27$ in each group. $^*p < .05$. **(H, I)** The SI time of stressed mice injected with AAV-control was significantly lower than that of nonstressed mice injected with AAV-control **(H)**, whereas this reduction was prevented in mice injected with AAV-Cartpt **(I)**. $n = 12–16$ in each group. $^*p < .05$. All data are presented as mean ± SEM. AAV, adeno-associated virus; aCC, anterior cingulate cortex; EGFP, enhanced green fluorescent protein; FST, forced swim test; GABAergic, gamma-aminobutyric acidergic; inj., injection; NS, nonstress control; n.s., not significant; SIT, social interaction test; smSDS, subchronic and mild social defeat stress.

inducing a depression-like phenotype in the BALB strain (23). We found significantly decreased FST immobility time (Figure 5F) but comparable SI time in SIT-1 (Figure 5G) in mice injected with AAV-Gad1-Cartpt relative to AAV-Gad1-mCherry. After subchronic and mild social defeat stress SDS exposure, mice injected with AAV-Gad1-mCherry showed a significant reduction in SI time (Figure 5H), whereas mice injected with AAV-Gad1-Cartpt showed an SI time that was comparable to that of nonstressed animals (Figure 5I). These results suggest

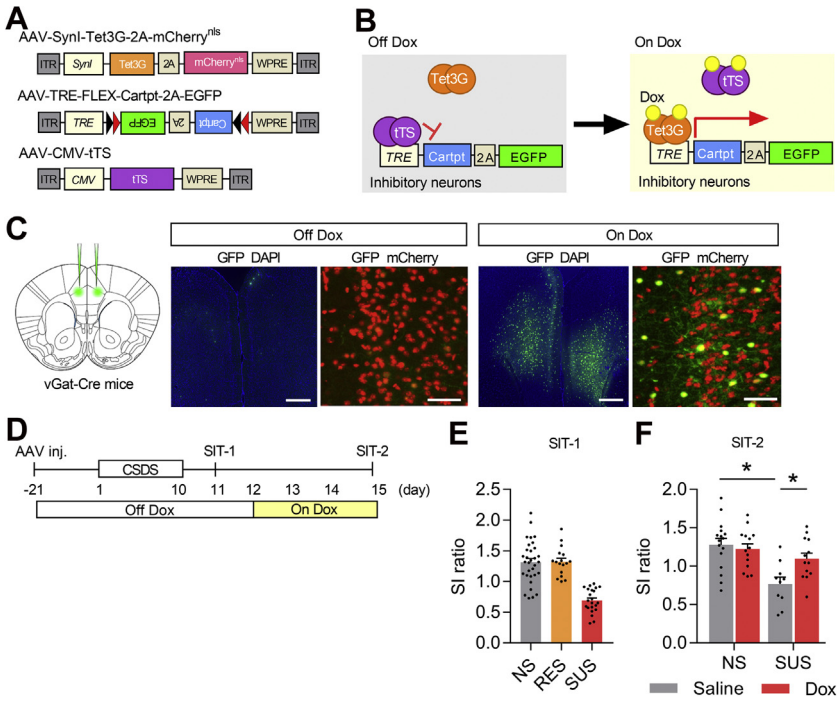

Figure 6. CART peptides in GABAergic neurons of the aCC have an antidepressant effect in stress-susceptible mice. **(A)** AAV-mediated spatiotemporal gene expression strategy using a cocktail of AAV-SynI-Tet3G-2A-mCherry^{nls}, AAV-TRE-FLEX-Cartpt-2A-EGFP, and AAV-CMV-tTS. **(B)** Schematic representation of dox- and Cre-dependent regulation of TRE-mediated gene expression in the inhibitory neurons using both the tetracycline-dependent activator (Tet3G) and repressor (tTS). Without dox, tTS represses TRE-mediated gene expression, whereas in the presence of dox, Tet3G activates TRE-mediated gene expression specifically in Cre-expressing cells. **(C)** AAV microinjection into the aCC region of vGat-Cre mice. Region-specific and dox-regulated expression of mCherry in the aCC is shown. Scale bar = 500 μm for low-magnification images (GFP and DAPI) and 50 μm for high-magnification images (GFP and mCherry). **(D)** Experimental timeline of *Cartpt* induction in inhibitory neurons of the aCC after the termination of CSDS episodes. Mice injected with a cocktail of AAVs were subjected to 10-day CSDS and were tested by SIT-1, followed by the administration of dox for 3 days (twice per day). Mice were tested using a SIT-2. **(E)** SI ratio after CSDS exposure (SIT-1). The CSDS group was divided into two groups (RES and SUS groups) based on their SI ratios. n = 32 for NS and 39 for CSDS (both RES and SUS). **(F)** SI ratio before (SIT-1) and after (SIT-2) dox administration in NS and SUS mice. CART peptide induction did not affect the SIT in nonstressed conditions, whereas the reduced SIT in SUS mice was rescued by CART peptide induction with dox. n = 10–14 in each group. *$p < .05$. All data are presented as mean ± SEM. AAV, adeno-associated virus; aCC, anterior cingulate cortex; CSDS, chronic social defeat stress; dox, doxycycline; EGFP, enhanced green fluorescent protein; GABAergic, gamma-aminobutyric acid-ergic; inj., injection; NS, nonstress control; RES, resilience; SIT, social interaction test; SUS, susceptible.

that CART peptide induction in the GABAergic neurons of the aCC drives antidepressant-like behavior and stress resilience independently of genetic background.

Antidepressant-like Effect of CART Peptide Induction in an Animal Model of Stress-Induced Depression

Because CART peptide induction before and during stress episodes prevented stress-induced depression-like behaviors (Figures 4 and 5), we tested whether CART peptide overexpression after stress induction reversed depression-like behaviors. We used a tetracycline system to overexpress CART peptides after the termination of CSDS episodes. We injected a cocktail of AAVs expressing a tetracycline-dependent transcription activator (Tet3G) under the control of the *SynI* promoter (AAV-SynI-tet3G-2A-mCherry^{nls}), together with a Cre- and tetracycline-dependent AAV expressing CART peptide and EGFP (AAV-TRE-FLEX-Cartpt-2A-EGFP) and an AAV expressing a tetracycline-dependent transcription silencer (AAV-CMV-tTS), into the aCC of vGat-Cre mice (Figure 6A). In this system, tTS represses TRE-mediated gene expression (i.e., *Cartpt* and *Egfp*) in the absence of doxycycline (dox), whereas in the presence of dox, Tet3G activates TRE-mediated gene expression specifically in Cre-expressing Gad1 neurons (Figure 6B). For verification, we performed histological analysis; a GFP signal was observed in mCherry-positive neurons in a dox-dependent manner (Figure 6C). We then subjected AAV-injected mice to CSDS, performed SIT, and classified them as susceptible (SUS) and resilient mice (Figure 6D) based on their SI ratio with a cutoff value: mice with an SI ratio of <1 were labeled as SUS and those with an SI ratio of >1 as resilient, as reported previously (24) (Figure 6E). After CSDS exposure, SUS and nonstressed mice were treated with dox for 3 days to induce transgene expression, followed by SIT (Figure 6D). We found that CART peptide induction by dox treatment in SUS mice after CSDS episodes showed significantly increased SI time in SIT-2, when compared with saline-treated SUS mice (Figure 6F). These data suggest that CART peptide induction in Gad1 neurons of the aCC is sufficient for inducing antidepressant response.

DISCUSSION

Investigating antidepressant-induced transcriptional changes in responders and nonresponders can help distinguish drug-induced therapeutic changes from off-target effects (16,36). We found fundamental differences in the transcription signatures of antidepressant responders and nonresponders. In addition to the individual differences within a given genetic background, it is known that phenotypic responses often vary depending on genetic backgrounds (37) and that the genetic background influences a behavioral response to antidepressants in mice (17–19). Although responses to antidepressants in clinical depression vary (1), a limited number of preclinical studies have mentioned the issue of heterogeneity observed in antidepressant responses (16,36). Herein, we used an experimental strategy to identify a specific molecule responsible for

antidepressant responses among multiple antidepressant drugs that is independent of genetic background; this approach may be informative in terms of translational research and drug development. We identified the CART peptide as a common molecule underlying antidepressant response, suggesting that it is a strong candidate for use in treating depression.

We investigated whether a common set of genes is regulated in the same way in BALB mice treated with two classes of antidepressants (i.e., selective serotonin reuptake inhibitors and selective noradrenaline reuptake inhibitors). Most of the regulated genes differed between these classes and between responders and nonresponders. Only seven genes, including immediate early genes (*c-fos*, *Egr1*, and *Egr2*), were consistently upregulated in responders and nonresponders to SRT and DLX (Figure 2B). Because enhanced immediate early gene expression is thought to be associated with high neuronal activity, our data suggest that certain cell populations within the mPFC respond to antidepressants regardless of behavioral alterations.

We found that unlike the expression of immediate early genes, *Cartpt* is a common gene upregulated in antidepressant responders of multiple strains and different types of antidepressants. Thus, *Cartpt* expression could be a molecular marker for antidepressant-like behavioral effects, instead of *c-fos* expression, at least in the aCC region. CART peptides are implicated in a wide range of physiological and behavioral functions, including stress response, appetite, sexual behavior, sleep, reward, autonomic regulation, and endocrine control (38–41). Deficits in these functions are often associated with depression symptoms, suggesting the key role played by CART peptides in depression. In humans, a small cohort with the Leu34Phe missense mutation in *CARTPT*, which leads to CART peptide deficiency (42), exhibited higher anxiety and depression scores (43). In rodents, exposure to chronic mild stress was associated with downregulation of *Cartpt* mRNA expression in the frontal cortex (44), and the electroconvulsive stimulation, used for treatment-resistant depression, upregulated *Cartpt* mRNA and protein expression in the nucleus accumbens of rats (45). Our study provides previously missing, precise, and cell type–specific roles of CART peptides in behavioral regulation, such as anxiety, SI, active escape behavior, and anhedonia, in response to antidepressant treatment. Thus, CART peptide could be, at least in the aCC area, an endogenous antidepressant.

Our data indicated that the expression of *Cartpt* was increased in the aCC of antidepressant-responder mice and that the aCC-specific overexpression of CART peptide promoted antidepressant-like behavioral response, suggesting a possible contribution of the aCC to the behavioral response to antidepressants. It is important to compare homologous sites to synthesize the findings in rodents and humans, but the most commonly used partitioning of the rodent aCC is inconsistent with that of humans (46). In addition, there is a discrepancy in the cross-species definition of the aCC (46–48). Nevertheless, the site we have targeted in this study (corresponding to the anterior part of Brodmann area 24 in humans) can be regarded as the aCC by any definitions. Multiple clinical studies have suggested that the aCC is involved in the pathophysiology of depression (49–52). Preclinical studies also revealed that structural plasticity within the aCC plays a critical role in the rapid antidepressant-like behavior afforded by ketamine and psilocybin (13,53). These results support our notion that aCC function could be associated with promoting behavioral responses to antidepressants and stress resiliency.

We also identified a GABAergic neuron–specific role of CART peptides in antidepressant effects. The involvement of PFC GABA-related genes has been suggested in MDD pathophysiology (8,9,54), supporting a recent single-nucleus transcriptomics analysis of the postmortem PFC in MDD, which suggests that cortical neuron subtypes are involved in depression (10). Enhanced cortical GABA levels in MDD could be a potential mechanism underlying the treatment effects of typical antidepressants, ketamine, repetitive transcranial magnetic stimulation, and electroconvulsive therapy (55–58). Preclinical studies have demonstrated that the regulation of depression-related and antidepressant-like behaviors depends on the interneuron subtype targeted within the mPFC and/or aCC (59–61). Thus, abundant evidence supports the notion that the cortical GABAergic system is a key regulator of stress-induced behavioral changes and antidepressant-like behaviors. Although how CART peptides modulate GABA neurotransmission in the aCC remains unknown, the interaction between CART peptides and GABA signals might provide critical clues regarding the mechanism of action of antidepressants.

This study has several limitations. We used only male mice; therefore, our results are not necessarily generalizable to female mice. Given that previous evidence suggests sex-specific transcriptome changes in MDD and differences in antidepressant responsiveness between genders (62–64), further studies are necessary. Nonetheless, our study provides important information for subsequent studies aimed at exploring both male and female antidepressant responders. We found individual *Cartpt* expression differences in the antidepressant treatment response, whereas the underlying mechanisms remain unclear. Although a genetic component might account for the antidepressant response (20,65), it has been suggested that MDD and treatment responses result from genetic and environmental interactions. Such interactions could be mediated by epigenetic mechanisms and we speculate that differential epigenetic marks on the *Cartpt* gene, along with environmental and genetic factors, might influence its transcription and determine the behavioral response to antidepressants. Future work would be required to delineate the relative contribution of epigenetic, genetic, and environmental factors that might explain together the variations in the role the antidepressants play. It will also be important to determine how the CART peptide–dependent signal exerts antidepressant-like behaviors. These studies remained limited by absence of any identified CART peptide receptors. However, recent reports have identified two orphan receptors, GPR68 and GPR160, as putative receptors for CART peptides (66,67). Although it remains unclear whether CART peptides can stimulate these G protein–coupled receptors in the brain, understanding these receptors, their interaction with CART peptides, and their roles in mood and emotion may provide novel insights for the treatment of psychiatric disorders.

In conclusion, our data suggest that CART peptide signaling in GABAergic neurons of the aCC might be a common

molecular mechanism across antidepressant responders independent of genetic backgrounds and that this pathway also drives stress resilience. This study may provide a strategy for identifying novel drug targets and developing approaches that positively modulate CART peptide signaling represents a promising avenue for treating depression.

ACKNOWLEDGMENTS AND DISCLOSURES

This work was supported by the Japan Society for the Promotion of Science (KAKENHI Grant Nos. JP18H02750, JP21K19707, JP21H02849, JP21K15711, and JP21K07593), the Ministry of Education, Culture, Sports, Science and Technology (KAKENHI Grant No. JP21H00198), and the Agency for Medical Research and Development (Grant Nos. JP20ak0101136 and JP21dm0307102h0003).

YF, NO, and SU designed the study. YF, HL, AK-K, EI, HI, HY, TS, and SU performed the experiments. NO and SU analyzed RNA sequencing data. SN and YW provided critical reagents. YF, NO, and SU wrote the manuscript with input from TM.

We thank Mr. Naoto Yasuda, Ms. Ayumi Kobayashi, Ms. Kaede Kuroda, and Ms. Kumiko Hara for technical assistance.

The authors report no biomedical financial interests or potential conflicts of interest.

ARTICLE INFORMATION

From the SK Project (YF, HL, EI, AK-K, HI, TM, NO, SU), Medical Innovation Center; Department of Psychiatry (YF, HI, TM), Kyoto University Graduate School of Medicine, Kyoto; and the Division of Neuropsychiatry (HY, TS, SN, YW), Department of Neuroscience, Yamaguchi University Graduate School of Medicine, Yamaguchi, Japan.

YW is currently affiliated with Southern TOHOKU Research Institute for Neuroscience, Southern TOHOKU General Hospital, Koriyama, Japan.

Address correspondence to Shusaku Uchida, Ph.D., at uchida.shusaku.3n@kyoto-u.ac.jp, or Naoya Oishi, M.D., Ph.D., at noishi@kuhp.kyoto-u.ac.jp.

Received Oct 7, 2021; revised Dec 9, 2021; accepted Dec 27, 2021.

Supplementary material cited in this article is available online at https://doi.org/10.1016/j.bpsgos.2021.12.009.

REFERENCES

1. Rush AJ, Trivedi MH, Wisniewski SR, Nierenberg AA, Stewart JW, Warden D, *et al.* (2006): Acute and longer-term outcomes in depressed outpatients requiring one or several treatment steps: A STAR*D report. Am J Psychiatry 163:1905–1917.
2. Pizzagalli DA, Roberts AC (2022): Prefrontal cortex and depression [published correction appears in Neuropsychopharmacology 2022; 47: 609]. Neuropsychopharmacology 47:225–246.
3. Ploski JE, Vaidya VA (2021): The neurocircuitry of posttraumatic stress disorder and major depression: Insights into overlapping and distinct circuit dysfunction-A tribute to Ron Duman. Biol Psychiatry 90:109–117.
4. Krishnan V, Nestler EJ (2010): Linking molecules to mood: New insight into the biology of depression. Am J Psychiatry 167:1305–1320.
5. Drevets WC (2000): Functional anatomical abnormalities in limbic and prefrontal cortical structures in major depression. Prog Brain Res 126:413–431.
6. Mayberg HS, Liotti M, Brannan SK, McGinnis S, Mahurin RK, Jerabek PA, *et al.* (1999): Reciprocal limbic-cortical function and negative mood: Converging PET findings in depression and normal sadness. Am J Psychiatry 156:675–682.
7. Duman RS, Aghajanian GK (2012): Synaptic dysfunction in depression: Potential therapeutic targets. Science 338:68–72.
8. Girgenti MJ, Wang J, Ji D, Cruz DA, Traumatic Stress Brain Research Group, Stein MB, *et al.* (2021): Transcriptomic organization of the human brain in post-traumatic stress disorder. Nat Neurosci 24:24–33.
9. Sequeira A, Mamdani F, Ernst C, Vawter MP, Bunney WE, Lebel V, *et al.* (2009): Global brain gene expression analysis links glutamatergic and GABAergic alterations to suicide and major depression. PLoS One 4:e6585.
10. Nagy C, Maitra M, Tanti A, Suderman M, Théroux JF, Davoli MA, *et al.* (2020): Single-nucleus transcriptomics of the prefrontal cortex in major depressive disorder implicates oligodendrocyte precursor cells and excitatory neurons. Nat Neurosci 23:771–781.
11. Duman RS, Sanacora G, Krystal JH (2019): Altered connectivity in depression: GABA and glutamate neurotransmitter deficits and reversal by novel treatments. Neuron 102:75–90.
12. Covington HE 3rd, Lobo MK, Maze I, Vialou V, Hyman JM, Zaman S, *et al.* (2010): Antidepressant effect of optogenetic stimulation of the medial prefrontal cortex. J Neurosci 30:16082–16090.
13. Moda-Sava RN, Murdock MH, Parekh PK, Fetcho RN, Huang BS, Huynh TN, *et al.* (2019): Sustained rescue of prefrontal circuit dysfunction by antidepressant-induced spine formation. Science 364: eaat8078.
14. Ferenczi EA, Zalocusky KA, Liston C, Grosenick L, Warden MR, Amatya D, *et al.* (2016): Prefrontal cortical regulation of brainwide circuit dynamics and reward-related behavior. Science 351:aac9698.
15. Uchida S, Hara K, Kobayashi A, Funato H, Hobara T, Otsuki K, *et al.* (2010): Early life stress enhances behavioral vulnerability to stress through the activation of REST4-mediated gene transcription in the medial prefrontal cortex of rodents. J Neurosci 30:15007–15018.
16. Bagot RC, Cates HM, Purushothaman I, Vialou V, Heller EA, Yieh L, *et al.* (2017): Ketamine and imipramine reverse transcriptional signatures of susceptibility and induce resilience-specific gene expression profiles. Biol Psychiatry 81:285–295.
17. Dulawa SC, Holick KA, Gundersen B, Hen R (2004): Effects of chronic fluoxetine in animal models of anxiety and depression. Neuropsychopharmacology 29:1321–1330.
18. Schmidt EF, Warner-Schmidt JL, Otopalik BG, Pickett SB, Greengard P, Heintz N (2012): Identification of the cortical neurons that mediate antidepressant responses. Cell 149:1152–1163.
19. Crowley JJ, Brodkin ES, Blendy JA, Berrettini WH, Lucki I (2006): Pharmacogenomic evaluation of the antidepressant citalopram in the mouse tail suspension test. Neuropsychopharmacology 31:2433–2442.
20. Santarelli L, Saxe M, Gross C, Surget A, Battaglia F, Dulawa S, *et al.* (2003): Requirement of hippocampal neurogenesis for the behavioral effects of antidepressants. Science 301:805–809.
21. Uchida S, Hara K, Kobayashi A, Otsuki K, Yamagata H, Hobara T, *et al.* (2011): Epigenetic status of Gdnf in the ventral striatum determines susceptibility and adaptation to daily stressful events. Neuron 69:359–372.
22. Golden SA, Covington HE 3rd, Berton O, Russo SJ (2011): A standardized protocol for repeated social defeat stress in mice [published correction appears in Nat Protoc 2015; 10:643]. Nat Protoc 6:1183–1191.
23. Sakai Y, Li H, Inaba H, Funayama Y, Ishimori E, Kawatake-Kuno A, *et al.* (2021): Gene-environment interactions mediate stress susceptibility and resilience through the CaMKIIβ/TARPγ-8/AMPAR pathway. iScience 24:102504.
24. Krishnan V, Han MH, Graham DL, Berton O, Renthal W, Russo SJ, *et al.* (2007): Molecular adaptations underlying susceptibility and resistance to social defeat in brain reward regions. Cell 131:391–404.
25. Uchida S, Hara K, Kobayashi A, Fujimoto M, Otsuki K, Yamagata H, *et al.* (2011): Impaired hippocampal spinogenesis and neurogenesis and altered affective behavior in mice lacking heat shock factor 1. Proc Natl Acad Sci U S A 108:1681–1686.
26. Zanos P, Moaddel R, Morris PJ, Georgiou P, Fischell J, Elmer GI, *et al.* (2016): NMDAR inhibition-independent antidepressant actions of ketamine metabolites. Nature 533:481–486.
27. Casarotto PC, Girych M, Fred SM, Kovaleva V, Moliner R, Enkavi G, *et al.* (2021): Antidepressant drugs act by directly binding to TRKB neurotrophin receptors. Cell 184:1299–1313.e19.
28. Porsolt RD, Le Pichon M, Jalfre M (1977): Depression: A new animal model sensitive to antidepressant treatments. Nature 266:730–732.

29. David DJ, Samuels BA, Rainer Q, Wang JW, Marsteller D, Mendez I, *et al.* (2009): Neurogenesis-dependent and -independent effects of fluoxetine in an animal model of anxiety/depression. Neuron 62:479–493.
30. Trivedi MH, Rush AJ, Wisniewski SR, Nierenberg AA, Warden D, Ritz L, *et al.* (2006): Evaluation of outcomes with citalopram for depression using measurement-based care in STAR*D: Implications for clinical practice. Am J Psychiatry 163:28–40.
31. Laine MA, Trontti K, Misiewicz Z, Sokolowska E, Kulesskaya N, Heikkinen A, *et al.* (2018): Genetic control of myelin plasticity after chronic psychosocial stress. eNeuro 5: ENEURO.0166-18.2018.
32. Luo Y, Kataoka Y, Ostinelli EG, Cipriani A, Furukawa TA (2020): National prescription patterns of antidepressants in the treatment of adults with major depression in the US between 1996 and 2015: A population representative survey based analysis [published correction appears in Front Psychiatry 2020; 11:171]. Front Psychiatry 11:35.
33. Yu Z, Zhang J, Zheng Y, Yu L (2020): Trends in antidepressant use and expenditure in six major cities in China from 2013 to 2018. Front Psychiatry 11:551.
34. Doyle JP, Dougherty JD, Heiman M, Schmidt EF, Stevens TR, Ma G, *et al.* (2008): Application of a translational profiling approach for the comparative analysis of CNS cell types [published correction appears in Cell 2009; 139:1022]. Cell 135:749–1762.
35. Heiman M, Schaefer A, Gong S, Peterson JD, Day M, Ramsey KE, *et al.* (2008): A translational profiling approach for the molecular characterization of CNS cell types. Cell 135:738–748.
36. Carrillo-Roa T, Labermaier C, Weber P, Herzog DP, Lareau C, Santarelli S, *et al.* (2017): Common genes associated with antidepressant response in mouse and man identify key role of glucocorticoid receptor sensitivity. PLoS Biol 15:e2002690.
37. Sittig LJ, Carbonetto P, Engel KA, Krauss KS, Barrios-Camacho CM, Palmer AA (2016): Genetic background limits generalizability of genotype-phenotype relationships. Neuron 91:1253–1259.
38. Rogge G, Jones D, Hubert GW, Lin Y, Kuhar MJ (2008): CART peptides: Regulators of body weight, reward and other functions [published correction appears in Nat Rev Neurosci 2010; 11:218]. Nat Rev Neurosci 9:747–758.
39. Lau J, Herzog H (2014): CART in the regulation of appetite and energy homeostasis. Front Neurosci 8:313.
40. Singh A, de Araujo AM, Krieger JP, Vergara M, Ip CK, de Lartigue G (2021): Demystifying functional role of cocaine- and amphetamine-related transcript (CART) peptide in control of energy homeostasis: A twenty-five year expedition. Peptides 140:170534.
41. Ahmadian-Moghadam H, Sadat-Shirazi MS, Zarrindast MR (2018): Cocaine- and amphetamine-regulated transcript (CART): A multifaceted neuropeptide. Peptides 110:56–77.
42. Yanik T, Dominguez G, Kuhar MJ, Del Giudice EM, Loh YP (2006): The Leu34Phe ProCART mutation leads to cocaine- and amphetamine-regulated transcript (CART) deficiency: A possible cause for obesity in humans. Endocrinology 147:39–43.
43. Miraglia del Giudice E, Santoro N, Fiumani P, Dominguez G, Kuhar MJ, Perrone L (2006): Adolescents carrying a missense mutation in the CART gene exhibit increased anxiety and depression. Depress Anxiety 23:90–92.
44. Orsetti M, Di Brisco F, Canonico PL, Genazzani AA, Ghi P (2008): Gene regulation in the frontal cortex of rats exposed to the chronic mild stress paradigm, an animal model of human depression. Eur J Neurosci 27:2156–2164.
45. Roh MS, Cui FJ, Ahn YM, Kang UG (2009): Up-regulation of cocaine- and amphetamine-regulated transcript (CART) in the rat nucleus accumbens after repeated electroconvulsive shock. Neurosci Res 65:210–213.
46. van Heukelum S, Mars RB, Guthrie M, Buitelaar JK, Beckmann CF, Tiesinga PHE, *et al.* (2020): Where is cingulate cortex? A cross-species view. Trends Neurosci 43:285–299.
47. Bicks LK, Koike H, Akbarian S, Morishita H (2015): Prefrontal cortex and social cognition in mouse and man. Front Psychol 6:1805.
48. Vogt BA, Paxinos G (2014): Cytoarchitecture of mouse and rat cingulate cortex with human homologies. Brain Struct Funct 219:185–192.
49. Goldapple K, Segal Z, Garson C, Lau M, Bieling P, Kennedy S, Mayberg H (2004): Modulation of cortical-limbic pathways in major depression: Treatment-specific effects of cognitive behavior therapy. Arch Gen Psychiatry 61:34–41.
50. Goodman M, Hazlett EA, Avedon JB, Siever DR, Chu KW, New AS (2011): Anterior cingulate volume reduction in adolescents with borderline personality disorder and co-morbid major depression. J Psychiatr Res 45:803–807.
51. Youssef MM, Underwood MD, Huang YY, Hsiung SC, Liu Y, Simpson NR, *et al.* (2018): Association of BDNF Val66Met polymorphism and brain BDNF levels with major depression and suicide. Int J Neuropsychopharmacol 21:528–538.
52. Gibbons A, McPherson K, Gogos A, Dean B (2021): An investigation into nicotinic receptor involvement in mood disorders uncovers novel depression candidate genes. J Affect Disord 288:154–160.
53. Shao LX, Liao C, Gregg I, Davoudian PA, Savalia NK, Delagarza K, Kwan AC (2021): Psilocybin induces rapid and persistent growth of dendritic spines in frontal cortex in vivo. Neuron 109:2535–2544.e4.
54. Northoff G, Sibille E (2014): Why are cortical GABA neurons relevant to internal focus in depression? A cross-level model linking cellular, biochemical and neural network findings. Mol Psychiatry 19:966–977.
55. Sanacora G, Mason GF, Rothman DL, Krystal JH (2002): Increased occipital cortex GABA concentrations in depressed patients after therapy with selective serotonin reuptake inhibitors. Am J Psychiatry 159:663–665.
56. Sanacora G, Mason GF, Rothman DL, Hyder F, Ciarcia JJ, Ostroff RB, *et al.* (2003): Increased cortical GABA concentrations in depressed patients receiving ECT. Am J Psychiatry 160:577–579.
57. Dubin MJ, Mao X, Banerjee S, Goodman Z, Lapidus KAB, Kang G, *et al.* (2016): Elevated prefrontal cortex GABA in patients with major depressive disorder after TMS treatment measured with proton magnetic resonance spectroscopy. J Psychiatry Neurosci 41:E37–E45.
58. Milak MS, Proper CJ, Mulhern ST, Parter AL, Kegeles LS, Ogden RT, *et al.* (2016): A pilot in vivo proton magnetic resonance spectroscopy study of amino acid neurotransmitter response to ketamine treatment of major depressive disorder. Mol Psychiatry 21:320–327.
59. Fogaça MV, Wu M, Li C, Li XY, Picciotto MR, Duman RS (2021): Inhibition of GABA interneurons in the mPFC is sufficient and necessary for rapid antidepressant responses. Mol Psychiatry 26:3277–3291.
60. Fuchs T, Jefferson SJ, Hooper A, Yee PH, Maguire J, Luscher B (2017): Disinhibition of somatostatin-positive GABAergic interneurons results in an anxiolytic and antidepressant-like brain state. Mol Psychiatry 22:920–930.
61. Perova Z, Delevich K, Li B (2015): Depression of excitatory synapses onto parvalbumin interneurons in the medial prefrontal cortex in susceptibility to stress. J Neurosci 35:3201–3206.
62. Labonté B, Engmann O, Purushothaman I, Menard C, Wang J, Tan C, *et al.* (2017): Sex-specific transcriptional signatures in human depression [published correction appears in Nat Med 2018; 24:525]. Nat Med 23:1102–1111.
63. Kawatake-Kuno A, Murai T, Uchida S (2021): The molecular basis of depression: Implications of sex-related differences in epigenetic regulation. Front Mol Neurosci 14:708004.
64. Kornstein SG, Schatzberg AF, Thase ME, Yonkers KA, McCullough JP, Keitner GI, *et al.* (2000): Gender differences in treatment response to sertraline versus imipramine in chronic depression. Am J Psychiatry 157:1445–1452.
65. Uhr M, Tontsch A, Namendorf C, Ripke S, Lucae S, Ising M, *et al.* (2008): Polymorphisms in the drug transporter gene ABCB1 predict antidepressant treatment response in depression. Neuron 57:203–209.
66. Foster SR, Hauser AS, Vedel L, Strachan RT, Huang XP, Gavin AC, *et al.* (2019): Discovery of human signaling systems: Pairing peptides to G protein-coupled receptors. Cell 179:895–908.e21.
67. Yosten GL, Harada CM, Haddock C, Giancotti LA, Kolar GR, Patel R, *et al.* (2020): GPR160 de-orphanization reveals critical roles in neuropathic pain in rodents. J Clin Invest 130:2587–2592.